



PAPER

Fisher information rates in sequentially measured quantum systems

OPEN ACCESS

RECEIVED

18 January 2024

REVISED

5 March 2024

ACCEPTED FOR PUBLICATION


15 March 2024

PUBLISHED

27 March 2024

Original Content from
this work may be used
under the terms of the
[Creative Commons
Attribution 4.0 licence](#).

Any further distribution
of this work must
maintain attribution to
the author(s) and the title
of the work, journal
citation and DOI.

Eoin O'Connor^{1,2} , Steve Campbell^{1,2,3,*}  and Gabriel T Landi⁴ ¹ School of Physics, University College Dublin, Belfield, Dublin 4, Ireland² Centre for Quantum Engineering, Science, and Technology, University College Dublin, Belfield, Dublin 4, Ireland³ Dahlem Center for Complex Quantum Systems, Freie Universität Berlin, Arnimallee 14, 14195 Berlin, Germany⁴ Department of Physics and Astronomy, University of Rochester, Rochester, NY 14627, United States of America

* Author to whom any correspondence should be addressed.

E-mail: steve.campbell@ucd.ie**Keywords:** Fisher information, metrology, thermometry**Abstract**

We consider the impact that temporal correlations in the measurement statistics can have on the achievable precision in a sequential metrological protocol. In this setting, and for a single quantum probe, we establish that it is the transitions between the measurement basis states that plays the most significant role in determining the precision, with the resulting conditional Fisher information being interpretable as a rate of information acquisition. Projective measurements are shown to elegantly demonstrate this in two disparate estimation settings. Firstly, in determining the temperature of an environment and, secondly, to ascertain a parameter of the system Hamiltonian. In both settings we show that the sequential estimation approach can provide a useful method to enhance the achievable precision.

1. Introduction

Accurate measurements underpin our ability to understand all physical systems and processes. This places a high priority on the development of useful metrological protocols, i.e. estimation schemes to infer the maximal amount of information regarding some unknown parameters of a given system of interest. More formally, an estimation scheme is a process that converts measurement data into an estimate of an unknown parameter, θ . The Cramér–Rao bound [1, 2] places a lower bound on the variance of any unbiased estimation scheme

$$\sigma_{\theta} \geq \frac{1}{F_{\theta}}, \quad (1)$$

where F_{θ} is the associated Fisher information [3]. In standard quantum and classical estimation schemes the Fisher information scales linearly with the number of measurement results, N , leading to a N^{-1} scaling in the variance. By making use of quantum correlations, such as entanglement, between different sub-systems it is possible for quantum estimation schemes to achieve N^{-2} scaling, the so-called Heisenberg limit [4–7]. It has recently been demonstrated that it may even be possible to surpass the Heisenberg limit by exploiting critical phenomena [8–14].

In spite of the advantages, when dealing with quantum systems additional subtleties must be taken into account; such as the freedom in choosing the measurement basis or considering generalized measurement operators. In probe based metrology, where a sensor is placed in contact with a sample whose properties we wish to learn, measurement back-action can also play a significant role [15–20]. In fact, even if the sample is sufficiently large that the interaction between it and probe has negligible impact on its state, such back-action can still play a significant role in the effectiveness of the protocol depending on how the measurements are performed on the probe. If the *same* probe system is measured repeatedly, the backaction can cause each measurement result to depend on the outcomes of, in principle all, previous measurements. While the impact of this can be neglected if, as is often assumed, the probe is reset after each measurement, this has the

deleterious effect of making the process slow and, more importantly, potentially throwing away the opportunity to extract a better estimation by using the additional information gained due to the correlations established between the outcomes. This is motivation behind sequential quantum metrological protocols [21–26]. Additionally, if the probe is reset between each measurement it also precludes us from exploiting any quantum correlations that may have built up in our system and results in the Fisher information of such processes necessarily scaling linearly in the number of repetitions. There has been recent numerical evidence that it is possible to achieve super-linear scaling as the number of repetitions of a sequential measurement process increases [27, 28]. Although this scaling likely only holds for a finite number of repetitions [29].

In the sequential setting the metrological process can be depicted as a time-series of outcomes, i.e. a stochastic process. Due to the measurement backaction, the outcomes will generally be correlated in time. These correlations can affect the rate at which we acquire information, however, as has recently been shown in [30, 31], these correlations are not always beneficial and can either speed up or slow down the acquisition of information. It is therefore highly relevant to critically assess how correlations in time impact the rate of learning and to develop schemes that leverage the measurement backaction to increase metrological precision.

In this work we take precisely this approach in probe-based metrology, where we consider a single system acting as the probe, which is interacting with a sample (hereafter referred to as the environment). The protocol involves performing sequential measurements on the probe at discrete time intervals that generate correlations between the measurements, which can be leveraged to increase the Fisher information. For a process with finite Markov order, the Fisher information will necessarily scale linearly in the long-time limit, in contrast to the large Markov order found, e.g. in continuous [32–38] and weak [39, 40] measurement schemes, which can make parameter estimation difficult [41]. We demonstrate that stroboscopically performing projective measurements on the probe, whose underlying dynamics is otherwise Markovian, leads to a Markov order-1 measurement scheme. This results in a significantly simpler optimal estimation protocol and clear evidence of the role that temporal correlations in the measurement outcomes can have on the resulting Fisher information, which we can interpret as the rate of information acquisition. The small Markov order allows for effective feedback control [42, 43] to be implemented simply by adjusting the time between measurements. We analyse this approach in two paradigmatic metrological settings, thermometry of a large environment and estimation of the Rabi frequency of a qubit.

2. Correlated Fisher information

We consider a general setup of a system, with initial state ρ_S interacting with an environment at a state ρ_E , via a unitary U . From the perspective of the system, this can be described by the completely positive trace-preserving map

$$\mathcal{E}_\theta(\rho_S) = \text{tr}_E \{ U(\rho_S \otimes \rho_E) U^\dagger \} = \sum_i K_i \rho_S K_i^\dagger, \quad (2)$$

where $\{K_i\}$ are Kraus operators satisfying $\sum_i K_i^\dagger K_i = \mathbf{I}$. In the most general setting, the state of the environment ρ_E and/or the unitary U depend on an unknown parameter θ which we wish to estimate. The channel \mathcal{E}_θ therefore transfers information about θ to the probe system's state. Such a setting encompasses several broad classes of dynamics, including the case of purely unitary dynamics of the system, which occurs when U is a tensor product of unitaries. It also captures the case of generic quantum channels defined only by the Kraus operators, i.e. cases where we only have access to θ -dependent K_i 's.

The basic task of probe-based metrology is to extract an estimate of θ from measurements of the system alone. That is, we perform a generalized measurement on the system described by a set of operators L_ω with outcomes ω . The probability of obtaining outcome ω is

$$p(\omega|\rho_S) = \text{Tr}(\rho_S M_\omega), \quad M_\omega = L_\omega^\dagger L_\omega, \quad (3)$$

and the state of the system, given that the outcome was ω , is updated as

$$\rho_S \rightarrow \mathcal{L}_\omega(\rho_S) = \frac{L_\omega \rho_S L_\omega^\dagger}{p(\omega|\rho_S)}, \quad (4)$$

where the channel \mathcal{L}_ω is now non-linear as it refers to a specific outcome ω .

Typical probe based metrological protocols involve the resetting the state of the system and environment after each measurement, making each outcome ω iid (independent and identically distributed). The variance σ_θ of any estimator is bounded by the Cramér–Rao bound

$$\sigma_\theta \geq \frac{1}{NF_\theta^{\text{iid}}}, \quad (5)$$

where F_θ^{iid} is the Fisher information associated with a single outcome

$$F_\theta^{\text{iid}} = \sum_{\omega \in \Omega} \frac{1}{p(\omega|\mathcal{E}_\theta(\rho_S))} \left(\frac{\partial}{\partial \theta} p(\omega|\mathcal{E}_\theta(\rho_S)) \right)^2. \quad (6)$$

Resetting leads to the inevitable linear scaling for an iid measurement protocol. Relaxing the requirement to reset the system, and therefore moving beyond the iid setting, leads to correlations being established between the measurement outcomes and we examine the impact that these correlations have on the resulting Fisher information in the remainder of this section.

2.1. Correlated outcomes

We consider a scenario where we sequentially measure the same probe [22, 23, 25, 44, 45], i.e. after each measurement is performed the same probe is made interact with the environment again. For ease of calculation, we assume that the environment is sufficiently large and therefore its state resets at each time as is the case for dynamics accurately captured under the Markov approximation, or when the environment is modelled by a suitable collision model [46, 47]. In practice, this is tantamount to the assumption that the same channel \mathcal{E}_θ is applied each time. Crucially however, while the environment's state remains the same, the sequential nature of the process means that the system's state at the start of each interaction cycle will depend on the result of the previous measurements. Therefore, the results of the measurements are correlated with each other.

We consider a process where we first measure the system according to equation (4), then apply the channel (2) and then repeat this sequence. This leads to a string of outcomes $\omega_{1:N} := (\omega_1, \dots, \omega_N)$. The state of the system conditioned on these N outcomes will then be given by

$$\rho_S(\omega_{1:N}) = \mathcal{E}_\theta \circ \mathcal{L}_{\omega_N} \dots \circ \mathcal{E}_\theta \circ \mathcal{L}_{\omega_1}(\rho_S^0), \quad (7)$$

where \circ denotes map composition. At each step, the probability of obtaining the next outcome ω_{n+1} given all previous outcomes $\omega_{1:n}$ is

$$p(\omega_{n+1}|\omega_{1:n}) = \text{Tr}(\rho_S(\omega_{1:n})M_{\omega_{n+1}}), \quad (8)$$

and the probability of observing a particular sequence $\omega_{1:N}$ is

$$P(\omega_{1:N}) = p(\omega_N|\omega_{1:N-1}) \dots p(\omega_2|\omega_1)p(\omega_1). \quad (9)$$

This therefore describes a correlated (and generally non-Markov) stochastic process.

The measure-evolve-repeat sequence provides sufficient versatility that we can naturally introduce a feedback mechanism where the applied channels \mathcal{E}_θ are assumed to be conditioned on the previous measurement outcome. This modifies equation (7) according to

$$\rho_S(\omega_{1:N}) = \mathcal{E}_\theta^{\omega_N} \circ \mathcal{L}_{\omega_N} \dots \circ \mathcal{E}_\theta^{\omega_1} \circ \mathcal{L}_{\omega_1}(\rho_S^0). \quad (10)$$

This feedback could be introduced, e.g. by assuming that the unitary U applied in equation (2) at each step depends on the previous measurement outcome. This can lead to more information about the parameter of interest allowing to increase the estimation precision over iid protocols, as we detail below and demonstrate with explicit examples.

To formalise our ideas, consider the map $\Phi_\omega(\rho)$ that represents one iteration of the sequential measurement process with a specific measurement outcome,

$$\Phi_\omega(\rho_S) = \mathcal{E}_\theta^\omega \circ \mathcal{L}_\omega \rho_S. \quad (11)$$

We assume that the unconditional channel $\Phi(\rho_S) \equiv \sum_\omega p(\omega|\rho_S)\Phi_\omega(\rho_S)$ has a unique steady-state, $\Phi(\pi) = \pi$. We remark that $P(\omega_{1:N})$ is still conditioned on the initial state of the system. However, as will become clear below, the choice of initial state plays only a small role in the sequential measurement scheme, and therefore

to simplify the dynamics we assume the probe's initial state is given by the steady state; i.e. $\rho_S^0 = \pi$, thus making the probability distribution $P(\omega_{1:N})$ 'stationary' [30].

Since the resulting stochastic process (9) is now correlated, the Cramér–Rao bound (5) becomes

$$\sigma_\theta \geq \frac{1}{F_\theta(\omega_{1:N})}, \quad (12)$$

where

$$F_\theta(\omega_{1:N}) = \sum_{\omega_1, \dots, \omega_N} \frac{1}{P(\omega_{1:N})} \left(\frac{\partial}{\partial \theta} P(\omega_{1:N}) \right)^2. \quad (13)$$

The computation of $F_\theta(\omega_{1:N})$ is, in general, quite difficult as it involves a high-dimensional summation. Recently, it was shown by some of us [30] that the calculation of equation (13) simplifies for processes having a finite Markov order \mathcal{M} , an assumption which is true in many cases of interest. It is also approximately true in cases with infinite Markov order, as one can often define some sufficiently high effective Markov order \mathcal{M}_{eff} [29]. For systems with a finite Markov order equation (13) reduces to

$$F_\theta(\omega_{1:N}) = F_\theta(\omega_{1:\mathcal{M}}) + (N - \mathcal{M}) F_\theta(\omega_{\mathcal{M}+1} | \omega_{1:\mathcal{M}}). \quad (14)$$

The first term is the Fisher information of a block of \mathcal{M} outcomes, while the second is the conditional Fisher information, defined as

$$F_\theta(\omega_{\mathcal{M}+1} | \omega_{1:\mathcal{M}}) = \sum_{\omega_1, \dots, \omega_{\mathcal{M}}} P(\omega_{1:\mathcal{M}}) \sum_{\omega_{\mathcal{M}+1}} \frac{(\partial_\theta p(\omega_{\mathcal{M}+1} | \omega_{1:\mathcal{M}}))^2}{p(\omega_{\mathcal{M}+1} | \omega_{1:\mathcal{M}})}. \quad (15)$$

The quantity $p(\omega_{\mathcal{M}+1} | \omega_{1:\mathcal{M}})$ is the probability of future outcomes given all the relevant past, i.e. up to the Markov order. Equation (15) is the Fisher information of this distribution averaged over all possible pasts. For $N \gg \mathcal{M}$, equation (14) shows that the dominant contribution to the Fisher information is given by $F_\theta(\omega_{1:N}) \simeq N F_\theta(\omega_{\mathcal{M}+1} | \omega_{1:\mathcal{M}})$. This therefore allows us to interpret the conditional Fisher information as a Fisher information rate

$$F_\theta(\omega_{\mathcal{M}+1} | \omega_{1:\mathcal{M}}) = \lim_{N \rightarrow \infty} \frac{F_\theta(\omega_{1:N})}{N}. \quad (16)$$

That is, it represents the effective Fisher information acquired per outcome. Notice that this is generally different from F_θ^{fid} , as defined in equation (6). In fact, as shown in [30], there is no general relation between the two quantities, and $F_\theta(\omega_{\mathcal{M}+1} | \omega_{1:\mathcal{M}})$ can be both smaller or larger than F_θ^{fid} depending on the problem in question.

2.2. Projective measurements

A particularly elegant and useful instance of this corresponds to when the measurement operators L_ω in equation (4) are projective measurements onto some basis $\{|k\rangle\}$. Since the projection erases all information about previous states, this corresponds to a Markov order $\mathcal{M} = 1$; that is, each measurement result only depends on the previous outcome, i.e. when the underlying dynamics adheres to the Markov approximation. The probability of obtaining each outcome reduces to $p(k | \rho_S) = \langle k | \rho_S | k \rangle$ and the channel $\Phi_\omega(\rho_S)$ in equation (11) simplifies to

$$\Phi_k(\rho_S) = \mathcal{E}_\theta^k(|k\rangle\langle k|). \quad (17)$$

Hence, the conditional probability (8) reduces to

$$P(k|k') = \langle k | \left[\mathcal{E}_\theta^{k'}(|k'\rangle\langle k'|) \right] | k \rangle. \quad (18)$$

This formula elegantly encompasses the relationship between the quantum channel \mathcal{E}_θ and the actual measurement record that is observed, which in this case has the form of a Markov chain. The steady-state of Φ_k is $\pi = \sum_k q_k |k\rangle\langle k|$ where q_k is the solution of the Markov equation

$$q_k = \sum_{k'} q_{k'} P(k|k'). \quad (19)$$

For Markov order-1 processes, equation (14) simplifies to [30]

$$F_{\theta}(k_1, \dots, k_N) = F_1 + (N-1)F_{2|1}, \quad (20)$$

where we introduce the slightly simpler notation $F_1 = \sum_k (\partial_{\theta} q_k)^2 / q_k$ for the Fisher information of the steady-state distribution q_k , and

$$F_{2|1} = \sum_{k'} q_{k'} \sum_k \frac{1}{P(k|k')} \left(\frac{\partial}{\partial \theta} P(k|k') \right)^2, \quad (21)$$

for the conditional Fisher information. This quantity is precisely the Fisher information rate in equation (16). Interestingly, this result shows that for projective measurements, the rate at which we acquire information is directly related to the Fisher information of the transition probabilities $P(k|k')$. For a Markov order 1 process, we learn about θ by observing the transitions. It is therefore clear that the correlations between measurement outcomes in a sequential protocol will have an impact on the attainable precision. In section 3 we demonstrate that these correlations can both enhance and hinder an estimation scheme, and subsequently in section 4 provide explicit examples of how they can be leveraged to boost the effectiveness of a given protocol.

3. Comparison to other strategies

The key insight arising from equation (20) is that for a metrological scheme employing sequential measurements on a single probe system, what matters for the acquisition of information are the *transitions* from $k' \rightarrow k$. This is clear from the fact that $F_{2|1}$ depends on $\partial_{\theta} P(k|k')$, i.e. on how sensitive the transitions are to changes in θ . Conversely, F_1 depends on $\partial_{\theta} q_k$. One would naturally be tempted to compare $F_{2|1}$ with F_1 , or to any other meaningful quantity. It turns out, however, that these comparisons are quite subtle and can, in fact, lead to incomplete or incorrect conclusions due to neglecting specific aspects of a given implementation. We now attempt to clarify this issue.

3.1. Comparing with F_{θ}^{iid} in equation (6)

A first, somewhat naive, choice would be to compare $F_{2|1}$ with the case where the outcomes are i.i.d. There are two possible ways one might obtain iid outcomes. The first is to have N copies of the probe and send each one individually through the channel \mathcal{E}_{θ} , equation (2). However, this introduces an arbitrariness on the choice of initial state ρ_S , which can in principle be prepared in any way. This leads to a clear problem in comparing with the sequential setup since the states in that case are only prepared once and subsequently evolve. The second is to obtain iid outcomes by resetting the state of the probe system after each measurement. This could mean, for example, coupling it to a heat bath after each measurement, hence erasing information about past outcomes. Once again, this introduces an arbitrariness as to how the reset occurs and an additional arbitrary parameter, which is the time it takes to re-prepare the system.

In [25], the authors compared their results with the iid scenario. In particular, they considered the situation in which the system was always re-prepared in specific states $|k'\rangle$. The corresponding Fisher information is then a single term in the sum appearing in equation (20),

$$F_{2|1=k'} := \sum_k \frac{1}{P(k|k')} \left(\frac{\partial}{\partial \theta} P(k|k') \right)^2. \quad (22)$$

It is clear from equation (21) that $F_{2|1}$ will be a convex sum of such quantities:

$$F_{2|1} = \sum_{k'} q_{k'} F_{2|1=k'}. \quad (23)$$

We can therefore have $F_{2|1=k'} \leq F_{2|1}$, depending on the particular choice of k' . The quantities $F_{2|1=k'}$ are useful, as they tell us which outcomes k' lead to higher information gains. However, if one is using just a single probe then the quantity in fact being sampled is $F_{2|1}$.

3.2. Comparison with F_1

Alternatively, we may be inclined to compare $F_{2|1}$ with F_1 . The former is the information contained in the transition probabilities $P(k|k')$ and the latter is the information contained in distribution q_k (equation (19)). However, this comparison is generally not fair since the q_k -information is not acquired over independent trials. Instead, it is determined sequentially in a single run. This subtle point was recently discussed by some

of us in [31] and can be clarified as follows. The actual data we have at hand is the string k_1, \dots, k_N . Estimation therefore proceeds by building a function $\hat{\theta}(k_1, \dots, k_N)$ to use as the estimator. For any (unbiased) estimator, the error for large N will be bounded by $1/(NF_{2|1})$.

To achieve this bound, however, we must use estimators that make use of the transitions. For example, suppose that the functional form of a specific transition reads $P(2|1) = f(\theta)$, for some function $f(\theta)$. Then a potential estimator could be constructed as follows: given a single string k_1, \dots, k_N , we count how many times $k=1$ was followed by $k=2$, and use this to build an estimate $\hat{P}(2|1)$ for the transition probability. The function $f^{-1}(\hat{P}(2|1))$ would then be an estimator of θ , which will generally be unbiased for large N . Since this estimator uses information about transitions, it *might* saturate the Cramér–Rao bound asymptotically, although there is no guarantee of this.

In practice, we might prefer to use simpler estimators. For example, we can build a histogram of the outcomes. That is, given a string k_1, \dots, k_N , where each k_i ranges over some alphabet $k_i \in \{1, \dots, d\}$, we can build a histogram counting how many times $k_i = 1$ is recorded, how many times $k_i = 2$ is recorded and so on. This is called the *empirical distribution* (ED) and is a form of data compression. It can be shown that the ED is an unbiased estimator of the steady-state probabilities q_k , and hence, naively, we might expect that the information associated to it should be F_1 . However this is not the case, as shown in [31]. The reason being that the data string k_1, \dots, k_N is *not* i.i.d. Instead, it is acquired sequentially on a single run. As a consequence, due to correlations between sequential outcomes, the resulting Fisher information is affected. The actual form for the Fisher information in the ED is described in [31].

The only way we would obtain an information rate given by F_1 is if we perform the same protocol as section 2.2, but only use data points spaced by a large distance $\Delta \gg 1$. That is, we would have to perform $N\Delta$ measurements, however, instead of building an estimator based on $k_1, \dots, k_{N\Delta}$, we discard intermediate data and build an estimator involving only $k_1, k_{\Delta+1}, k_{2\Delta+1}, \dots$. This, of course, is a terrible strategy since it involves throwing away valuable data.

3.3. Direct measurements on the environment

In our approach, information about a parameter of the environment is obtained by coupling it to a probe system via the map (2). Suppose that the only dependence on θ is in the environment's state ρ_E^θ . Then equation (2) represents a form of data compression; that is, information is lost when it is transferred from ρ_E^θ to ρ_S . A natural way to quantify the amount lost is to compute the quantum Fisher information of ρ_E , which already maximizes over all possible measurements on the environment. The resulting quantity must then necessarily exceed $F_{2|1}$. In reality, of course, this compression can be significant, for example if the environment is very large and the system is small. In appendix A we prove a stronger result: we consider a maximization only over measurements that have the same number of outcomes as the dimension of the system. We find that

$$F_{2|1} \leq F_\theta^{\text{iid}^*} \leq F(\rho_E, G_i^*), \quad (24)$$

where $F_\theta^{\text{iid}^*}$ is equation (6) maximised over all initial states and $\{G_i^*\}$ is the optimal POVM with the same number of measurement outcomes as the dimension of ρ_S . Hence, even restricting the number of outcomes in the environment, a direct measurement would still be better than using a probe. This agrees with the results of [48], which studied temperature estimation in thermal states.

3.4. Relation to collisional schemes

The sequential measurement approach shares several commonalities with the recently proposed framework of collisional thermometry [49–52]. Instead of performing the measurement on the system itself, an auxiliary system is used which interacts (collides) with the probe system and the measurement is subsequently made on this auxiliary system. For projective measurements performed immediately after the interaction, we find that the Fisher information is equivalent to the sequential measurement scheme. We assume that the system and colliding auxiliary unit are initially uncorrelated and evolve via a unitary interaction

$$\rho_{SC} = U(\rho_S \otimes \rho_C) U^\dagger, \quad (25)$$

after which we perform a measurement of the auxiliary unit in an arbitrary basis $\{|i\rangle\}$. The probability of getting a measurement result i is then given by

$$\begin{aligned}
P(i) &= \text{Tr}[\rho_{SC}(\mathbf{I}_S \otimes |i\rangle\langle i|)] \\
&= \text{Tr}_S \left[\sum_j F_{i,j} \rho_S F_{i,j}^\dagger \right] \\
&= \text{Tr}_S[\rho_S E_i],
\end{aligned} \tag{26}$$

where we have defined $F_{i,j} = \langle i|U|p_j\rangle$ with $|p_j\rangle$ an eigenvector of the auxiliary unit and $E_i = \sum_j F_{i,j}^\dagger F_{i,j}$. Through a similar analysis to the one in appendix A we can prove that $\{E_i\}$ is a POVM on ρ_S . Therefore, performing a measurement on the auxiliary unit immediately after interaction is equivalent to performing a (different) measurement on the system itself. In fact, Neumark's theorem [53] proves that any POVM on the system can be realised via a suitable projective measurement on a collisional unit. This may be a useful practical method of realising some more complicated forms of POVMs on the system. The collisional setup still provides some additional freedom to make use of initial correlations between measurements [50] or collective measurements on multiple collisional units but a significant advantage has yet to be demonstrated for these methods.

4. Applications

4.1. Precision thermometry

We now turn to applications of our formalism. First, we consider the case of quantum thermometry [54–60], where it is known that an advantage can be obtained by using quantum probes for low temperatures [61–63]. Nevertheless, estimation of thermal probes is limited by the thermal Fisher information [64] which is maximised by using a D level probe with a non-degenerate ground state and $(D-1)$ -degenerate excited states [64]. The Hamiltonian reads $H_p = e_0|e_0\rangle\langle e_0| + \sum_{i=1}^{D-1} e_i|e_i\rangle\langle e_i|$, with energy spacing $e_1 - e_0 = \Omega$. Following [64], we model the environment as a bosonic heat bath with a flat spectral density. In suitable limits, this leads to the following master equation

$$\frac{d\rho_S}{dt} = \mathbb{L}\rho_S = \gamma \sum_{i=1}^{D-1} \{(1 + \bar{n})\mathcal{D}[|e_0\rangle\langle e_i|] + \bar{n}\mathcal{D}[|e_i\rangle\langle e_0|]\} \rho_S, \tag{27}$$

where $\mathcal{D}[L]\rho = L\rho L^\dagger - \frac{1}{2}\{L^\dagger L, \rho\}$, γ is the system-environment coupling and $\bar{n} = 1/(e^{\hbar\Omega/k_B T} - 1)$ is the mean occupation number. Our goal will be to estimate the occupation \bar{n} , from which we can estimate T assuming Ω is fixed and known [14]. The map \mathcal{E} , equation (2), corresponds to the evolution $\rho_S(t) = \mathcal{E}(\rho_S(0)) = e^{\mathbb{L}\tau}\rho_S(0)$, up to a certain time τ . This defines the time between measurements and will be used as a free parameter of the model which can be optimized over to enhance the estimation precision. We will restrict to measurements in the energy basis, since this is known to be optimal in the case of incoherent states. As a consequence, the system remains diagonal throughout the protocol.

In the limit of infinite evolution time $\tau \rightarrow \infty$, the steady state of the master equation (27) is the Gibbs thermal state, with ground-state occupation $q_0 = \langle e_0|\rho_S^{ss}|e_0\rangle = \frac{1+\bar{n}}{1+D\bar{n}}$, and excited state occupation $q_i = \langle e_i|\rho_S^{ss}|e_i\rangle = \frac{\bar{n}}{1+D\bar{n}}$, for all states $i = 1, \dots, D-1$. In this limit the map \mathcal{E} completely resets the state of the system, causing the outcomes to become i.i.d. The corresponding Fisher information, which is the analog of equation (6), is given by

$$\begin{aligned}
\mathcal{F}_{\text{th}} &= \frac{1}{q_0} \left(\frac{\partial}{\partial \bar{n}} q_0 \right)^2 + (D-1) \frac{1}{q_1} \left(\frac{\partial}{\partial \bar{n}} q_1 \right)^2 \\
&= \frac{D-1}{\bar{n}(1+\bar{n})(1+D\bar{n})^2},
\end{aligned} \tag{28}$$

and is precisely the thermal Fisher information. Particular to this setup, equation (28) coincides with all of the comparison quantities in section 3, making it the logical benchmark for the correlated process.

Similar in spirit to the collisional thermometry scheme of [49], with sequential measurements we can exploit the additional information about temperature that is contained in the thermalization rates of the probe by relaxing the assumption that $\tau \rightarrow \infty$ between each measurement, therefore the probe only partially thermalizes after each measurement. The first step is to compute the transition probability $P(k|k')$ in equation (18), where $|k\rangle$ now corresponds to the energy basis $|e_k\rangle$ of the probe Hamiltonian. These probabilities can be explicitly calculated, as detailed in appendix B, and we find

$$P(0|0) = 1 - q_e(1-f) \tag{29}$$

$$P(i|0) = \frac{q_e(1-f)}{D-1} \tag{30}$$

$$P(0|i) = q_0(1-f) \tag{31}$$

$$P(i|j) = \frac{q_e(1-f) + f - g}{D-1}, \quad j \neq i \tag{32}$$

$$P(i|i) = g + P(i|j), \tag{33}$$

where we have defined the probability of finding the system in any of the excited states, $q_e = 1 - q_0$, as well as the functions $g = e^{-\gamma\tau(\bar{n}+1)}$ and $f = e^{-\gamma\tau(D\bar{n}+1)}$ which represent the two most relevant relaxation rates of the problem. We remark that these rates naturally depend both on the choice of τ , as well as on \bar{n} , but we omit these explicit dependences for clarity of notation. The steady-state of the Markov chain, equation (19) is given by the same equilibrium probabilities q_k defined above. This is not immediately obvious: while it certainly must hold true when $\tau \rightarrow \infty$, for finite times this is less evident. The rationale behind this is explained in detail in appendix B.

Using these results we can compute the conditional Fisher information rates $F_{2|1=k'}$ in equation (22). If the measurement outcome was $k' = 0$ (i.e. the system was found in the ground-state), then the Fisher information rate for the next measurement will be

$$F_{2|1=e_0} = \frac{[\partial_{\bar{n}}P(0|0)]^2}{P(0|0)} + (D-1) \frac{[\partial_{\bar{n}}P(0|1)]^2}{P(0|1)} \tag{34}$$

$$= \frac{(\partial_{\bar{n}}x)^2}{x(1-x)}, \tag{35}$$

where $x = q_e(1-f) = 1 - P(0|0)$ is the probability that, after observing the system in the ground state, it is excited to any of the excited states after a time τ . This conditional Fisher information rate is therefore the same as that of a binary random variable, where the system is either in the ground or in the excited state after a time τ , given that at time $t=0$ it was in the ground state. Similarly, we can calculate the conditional Fisher information rate given that the outcome was one of the excited states $i = 1, \dots, D-1$. From equation (22) it follows that

$$F_{2|1=e_i} = \frac{[\partial_{\bar{n}}P(0|1)]^2}{P(0|1)} + \frac{[\partial_{\bar{n}}P(1|1)]^2}{P(1|1)} + (D-2) \frac{[\partial_{\bar{n}}P(2|1)]^2}{P(2|1)}, \tag{36}$$

where the factor of $D-2$ represents the number of excited states the system can go to, other than i , given that it was initially detected in i . With some simplifications, the final expression reads

$$F_{2|1=e_i} = \frac{(\partial_{\bar{n}}y)^2}{y} + \frac{1}{D-1} \frac{[(\partial_{\bar{n}}y) - (D-2)(\partial_{\bar{n}}g)]^2}{1-y-(D-2)g} + \frac{D-2}{D-1} \frac{[(\partial_{\bar{n}}y + \partial_{\bar{n}}g)]^2}{1-y-g}, \tag{37}$$

where $y = 1 - x - f$. The first term is the Fisher information of the binary process $i \rightarrow 0$, the second is the rate for $i \rightarrow i$, and the third is the rate for $i \rightarrow j$ with $j \neq i$, weighted by the $D-2$ possible j 's.

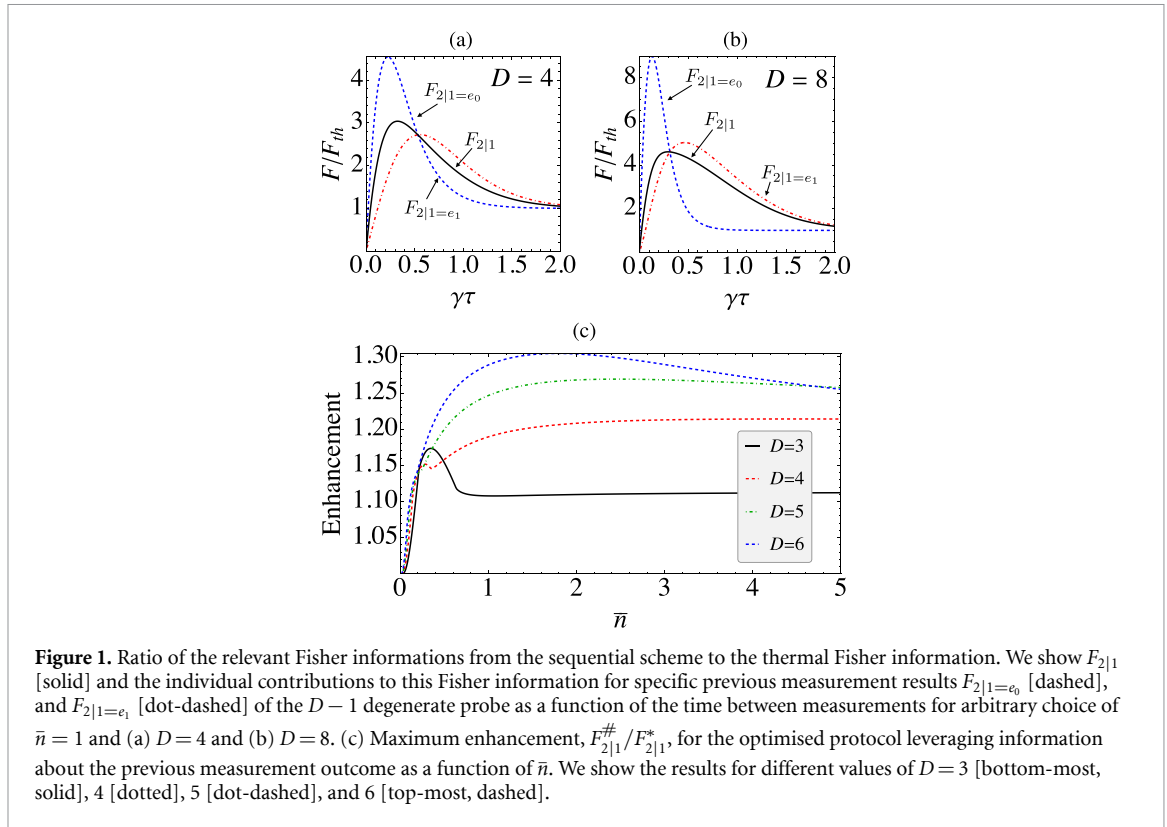
From these results, the total Fisher information rate in equation (20) is

$$F_{2|1} = q_0F_{2|1=e_0} + q_eF_{2|1=e_i}, \tag{38}$$

where, recall, $q_e = (D-1)q_i$. The quantities $F_{2|1=e_0}$, $F_{2|1=e_i}$ and $F_{2|1}$ are shown in figures 1(a) and (b) as a function of the measurement time $\gamma\tau$. We analyze the three different contributions, equations (35), (37) and (38) for $D=4$ and $D=8$. It is clear that there is an optimal finite time at which the Fisher information rates are maximized, i.e. partial thermalization is favorable as it allows us to gain more information about the temperature of the system from the relaxation rates. We can find this optimal Fisher information by calculating $F_{2|1}^* = \max_{\tau} F_{2|1}$ for any given value of \bar{n} .

From figure 1(a) it is clear that the value of the inter-measurement times $\gamma\tau$ which give the highest precision depend on whether the outcome was the ground or the excited state. Based on this, we can therefore envision a feedback mechanism that chooses the value of τ depending on the outcome. This would amount to using different values of τ in the probabilities (29)–(33). However, some care must be taken in doing so because the steady-state distribution q_k will no longer be the thermal distribution. As a consequence, the optimal times are not exactly the peaks of the dashed lines in figures 1(a) and (b). The new steady state probabilities are given by

$$q_0 = \frac{(1-f(\tau_g))\bar{n}}{1 + D\bar{n}(1-f(\tau_g)) + f(\tau_g)\bar{n} - (1+\bar{n})f(\tau_e)}. \tag{39}$$



To determine the maximal achievable precision we must optimise the combined Fisher information, equation (38), over both τ_e and τ_g , giving $F_{2|1}^{\#} = \max_{\tau_g, \tau_e} F_{2|1}$, which is a complex optimization problem which must be solved numerically. In figure 1(c) we show the enhancement achievable, i.e. $F_{2|1}^{\#}/F_{2|1}^*$, as a function of \bar{n} , which also scales with the increasing dimension of the probe. We find that the ratio of the optimal τ_g and τ_e changes very little with temperature implying that the feedback mechanism can reliably achieve this enhancement.

4.2. Thermometry with coarse grained energy measurements

Due to the degeneracy of the probe, there is a subtle distinction when we only have access to an energy measurement which is unable to distinguish between measurement outcomes in the degenerate eigenspace and which we will call partially indiscriminate, instead of the full measurement in the energy basis considered in section 4.1. The result of such a partially indiscriminate energy measurement would be the POVM

$$E_0 = |e_0\rangle\langle e_0|; \quad E_1 = \sum_{i=1}^{D-1} |e_i\rangle\langle e_i|. \quad (40)$$

Although this is no longer a projective measurement, the Fisher information still retains the same form as a projective measurement, i.e. that of equation (21). This is because the transition probability from one energy eigenspace to another is independent of the the specific state that the system is initially in within that subspace. The transition probabilities can be calculated in an analogous manner to the full energy basis measurement case detailed before and we find

$$P(0|0) = 1 - q_e(1 - f) \quad (41)$$

$$P(1|0) = q_e(1 - f) \quad (42)$$

$$P(0|1) = q_0(1 - f) \quad (43)$$

$$P(1|1) = 1 - q_0(1 - f). \quad (44)$$

As anticipated, the transition probabilities here are identical for transitions to the ground state and the transition probabilities to the excited subspace are simply the sum of all the transition probabilities to the individual excited energy eigenstates. The main difference now is that we are unable to distinguish measuring the *same* excited energy eigenstate two measurements in a row from measuring two different excited energy eigenstates. We can see the consequences of this difference in figure 2(a) and comparing it with figure 1(a).

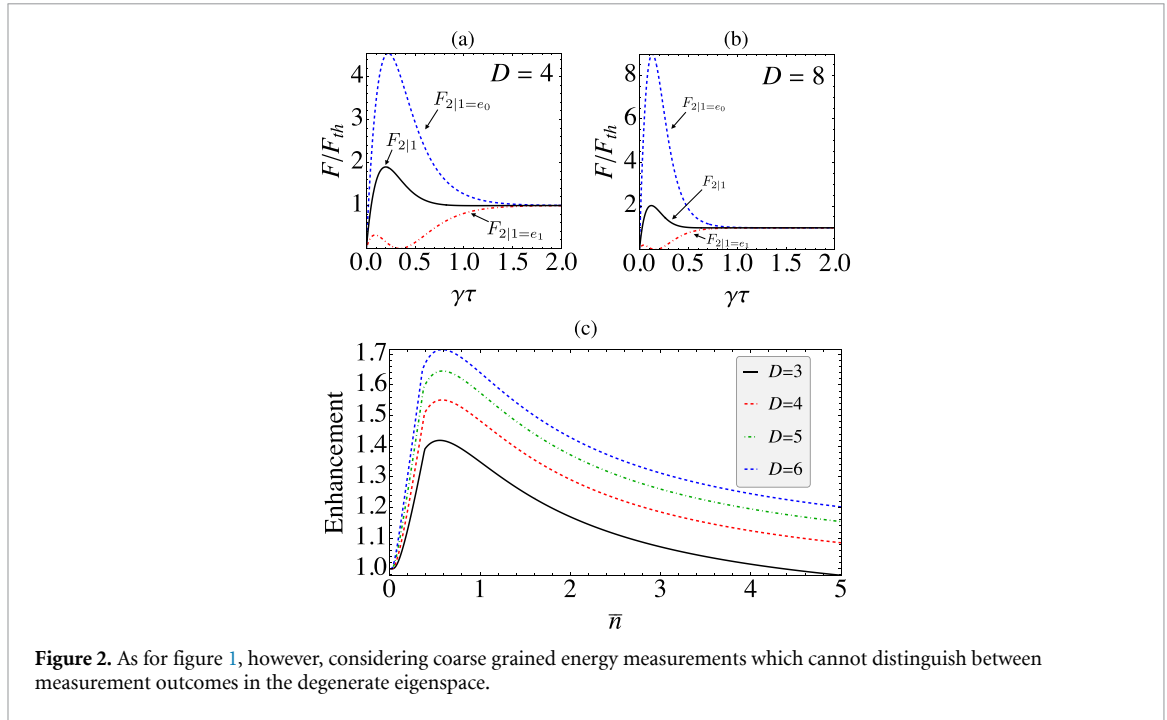


Figure 2. As for figure 1, however, considering coarse grained energy measurements which cannot distinguish between measurement outcomes in the degenerate eigenspace.

We see that the Fisher information is exactly the same when the previous measurement was a ground state (upper blue curve) but it is significantly lower for previous measurements that resulted in an excited state outcome due to the reduction in information we have for this measurement (bottom-most red dot-dashed curve). For low values of \bar{n} the Fisher information attainable when the previous measurement was excited is never larger than the thermal Fisher information. In this case an obvious measurement strategy to pursue would be to allow the system to fully thermalise after an excited energy measurement outcome is recorded and then optimise the Fisher information over the measurement time after a ground state measurement outcome is obtained. In fact, this is the optimal strategy for small \bar{n} and we can see in figure 2(c) that it can still provide a significant advantage over any strategy without feedback control.

This strategy indicates that there are other possible metrology protocols that, while not being projective measurements, nonetheless maintain the same form of the Fisher information as seen in equation (21). For equation (21) to hold, outcomes must depend only on the result of the directly preceding measurement. While projective measurements are an example of such a process, they are not the only example. As just discussed, we satisfy this condition if all of the POVM operators project onto degenerate subspaces. Additionally if we have POVM operators that project onto a non-degenerate subspace we could allow the system to fully equilibrate after obtaining that measurement result, the system will therefore be in the equilibrium state, independent of any previous measurements.

4.3. Rabi frequency estimation

We next demonstrate that the sequential metrology approach can be employed to determine a property of the system Hamiltonian, such as the Rabi frequency of a driven qubit [22], thus extending its applicability beyond estimating parameters of only the environment. To make our ideas concrete, we consider a qubit probe with Hamiltonian $H_S = \Omega\sigma_x$ which is coupled to an environment according to the master equation

$$\frac{d\rho_S}{dt} = \mathbb{L}\rho_S = -i[H, \rho_S] + \gamma\mathcal{D}[\sigma_-]\rho_S. \quad (45)$$

We once again consider sequential projective measurements in the system, with a free evolution of duration τ in between. Equation (18) then becomes

$$P(k|k') = \langle k| \left(e^{\mathbb{L}\tau} (|k'\rangle\langle k'|) \right) |k\rangle. \quad (46)$$

From this we can determine the steady-state distribution q_k in equation (19) and subsequently determine the conditional Fisher information rates $F_{2|1=k'}$ in equation (22), as well as its average $F_{2|1}$ in equation (21).

Figure 3 shows results for $F_{2|1=k'}$ and $F_{2|1}$ in the case of measurements in the computational basis $k' = \{|0\rangle, |1\rangle\}$ and we show the results for $\Omega/\gamma = 0.2$ in panel (a) and $\Omega/\gamma = 1.0$ in (b). The eigenvalues of

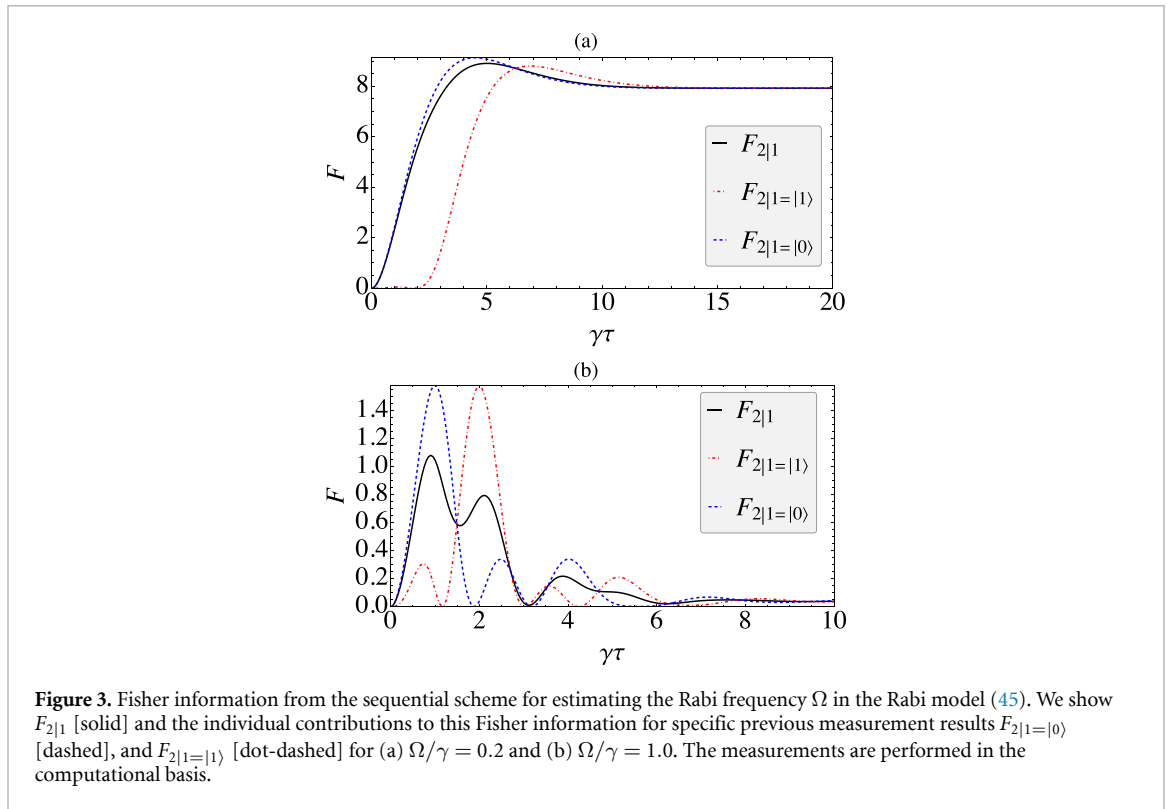


Figure 3. Fisher information from the sequential scheme for estimating the Rabi frequency Ω in the Rabi model (45). We show $F_{2|1}$ [solid] and the individual contributions to this Fisher information for specific previous measurement results $F_{2|1=|0\rangle}$ [dashed], and $F_{2|1=|1\rangle}$ [dot-dashed] for (a) $\Omega/\gamma = 0.2$ and (b) $\Omega/\gamma = 1.0$. The measurements are performed in the computational basis.

the Liouvillian depend on $\sqrt{\gamma^2 - 64\Omega^2}$, which becomes imaginary for $\Omega/\gamma > 1/8$. This is evident by comparing the behavior between the two settings in figure 3 as all Fisher rates show significantly more oscillations for larger Ω . We also see from the images that the information rates depend sensibly on τ , and this becomes particularly strong for large Ω/γ , cf figure 3(b), to the point where the Fisher information can actually be zero at certain points.

One could also study the same problem for bases in other directions. Measurements in the σ_x basis yield no information, while measurements in σ_y can and, in fact, generally do lead to somewhat larger Fisher information rates, although their behavior with $\gamma\tau$ is also different. Finally, one could ask about what is the optimal basis. However, this quickly becomes a difficult problem to solve in general since the basis will depend on the actual value of Ω , as well as on τ .

5. Conclusions

We have examined how temporal correlations established between measurement outcomes impact the achievable precision in estimating a parameter of interest using quantum probes. We considered a sequential measurement protocol, where the probe system is stroboscopically measured. We established that the resulting conditional Fisher information captures the rate at which information about the parameter of interest can be obtained. For protocols employing projective measurements, we have used our formalism to demonstrate that advantageous schemes can be developed. In the case of thermometry we showed that allowing for different waiting times between measurements of the probe based on the previous measurement outcomes allows for an increase in the achievable precision. Furthermore, we demonstrated that the protocol is versatile, allowing to effectively estimate Hamiltonian parameters such as the Rabi frequency. The latter example also established that the choice of measurement can play a significant role in the achievable precision, thus opening the possibility to explore whether further enhancement can be achieved by extending an adaptive scheme beyond allowing for different measurement times but also implementing measurements in a different basis at each step.

This work builds on [30, 31], which studied stochastic metrology of generic correlated outcomes in classical processes and connects those results with quantum processes. In particular, with the stochastic outcomes obtained when a quantum system is subject to stroboscopic measurements. Our work highlights the subtlety and care that must be considered when measurement outcomes in a metrological protocol are not independent and identically distributed. Furthermore, it provides a useful framework to explore a wider class of sensing protocols, in particular those that can leverage the temporal correlations to be more metrologically effective.

Data availability statement

All data that support the findings of this study are included within the article (and any supplementary files).

Acknowledgment

This work was supported by the Science Foundation Ireland Starting Investigator Research Grant ‘SpeedDemon’ No. 18/SIRG/5508 and the John Templeton Foundation Grant ID 62422. SC is grateful to the Alexander von Humboldt Foundation for their support.

Appendix A. Coarse grained comparison

We consider the setup from equation (2) of a general system-environment evolution with U and ρ_S independent of θ and $\rho_S = \sum_i s_i |s_i\rangle\langle s_i|$. When this is not the case it is possible to violate the following bound. The addition of an auxiliary system such as was considered in [48] has no effect on the following proof as long as the auxiliary system also has no θ dependence. Our first step is to derive the map $\mathcal{E}'(\rho_E) = \mathcal{E}(\rho_S)$

$$\begin{aligned}
 \mathcal{E}(\rho_S) &= \text{Tr}_E [U(\rho_S \otimes \rho_E) U^\dagger] \\
 &= \sum_i {}_E\langle b_i| U \left(\sum_j s_j |s_j\rangle\langle s_j|_S \otimes \rho_E \right) U^\dagger |b_i\rangle_E \\
 &= \sum_{i,j} s_j {}_E\langle b_i| U |s_j\rangle_S \rho_E |s_j\rangle_S U^\dagger |b_i\rangle_E \\
 &= \sum_{i,j} M_{i,j} \rho_E M_{i,j}^\dagger \\
 &= \mathcal{E}'(\rho_E),
 \end{aligned} \tag{A.1}$$

where $\{|b_i\rangle\}$ is an arbitrary basis of \mathcal{H}_E and $M_{i,j} = \sqrt{s_j} {}_E\langle b_i| U |s_j\rangle_S$. For the following analysis we require that $M_{i,j}$ is independent of θ with is clearly true when U and ρ_S are independent of θ but can also be true even when this is not the case. The quantum Fisher information of $\mathcal{E}(\rho_S)$ is then given by the Fisher information of $p_i(\mathcal{E}(\rho_S), E_i) = \text{Tr}[\mathcal{E}(\rho_S) E_i]$ maximised over all possible POVMs $\{E_i\}$. Where $\{E_i\}$ is a set of hermitian, positive semi-definite matrices that sum to the identity. Lets now look at the quantum Fisher information of $\mathcal{E}(\rho_S) = \mathcal{E}'(\rho_E) = \sum_j M_j \rho_E M_j^\dagger$. We will label the optimal POVM as $\{F_i\}$

$$\begin{aligned}
 p_i(\mathcal{E}(\rho_S), F_i) &= p_i(\mathcal{E}'(\rho_E), F_i) \\
 &= \text{Tr}[\mathcal{E}'(\rho_E) F_i] = \text{Tr} \left[\sum_{j,k} M_{j,k} \rho_E M_{j,k}^\dagger F_i \right] \\
 &= \sum_{j,k} \text{Tr} \left[M_{j,k} \rho_E M_{j,k}^\dagger F_i \right] = \sum_j \text{Tr} \left[\rho_E M_{j,k}^\dagger F_i M_{j,k} \right] \\
 &= \text{Tr} \left[\rho_E \left(\sum_{j,k} M_{j,k}^\dagger F_i M_{j,k} \right) \right].
 \end{aligned} \tag{A.2}$$

We can now define a new set of operators $G_i = \sum_{j,k} M_{j,k}^\dagger F_i M_{j,k}$, it is important to note that $\{G_i\}$ has the same number of elements as $\{F_i\}$. Now we need to prove that $\{G_i\}$ is a valid POVM on \mathcal{H}_E . Since F_i is Hermitian then G_i clearly is too. A matrix is positive semi-definite if and only if it can be decomposed into a product $F_i = L_i^\dagger L_i$. Since $\{F_i\}$ is a POVM we know that it can be decomposed. Therefore we can write $G_i = \sum_{j,k} M_{j,k}^\dagger L_i^\dagger L_i M_{j,k} = \sum_{j,k} K_{i,j,k}^\dagger K_{i,j,k}$ with $K_{i,j,k} = L_i M_{j,k}$. This means G_i is the sum of positive semi-definite matrices and is therefore also positive semi-definite. The last thing to show is that $\{G_i\}$ sums to the identity

$$\begin{aligned}
\sum_i G_i &= \sum_i \sum_{j,k} M_{j,k}^\dagger F_i M_{j,k} \\
&= \sum_{j,k} M_{j,k}^\dagger \left(\sum_i F_i \right) M_{j,k} = \sum_{j,k} M_{j,k}^\dagger M_{j,k} \\
&= \sum_{j,k} s_k s \langle s_k | U^\dagger | b_j \rangle_E \langle b_j | U | s_k \rangle_S \\
&= \sum_k s_k s \langle s_k | U U^\dagger | s_k \rangle_S \\
&= \mathbf{I}_E.
\end{aligned} \tag{A.3}$$

This implies that the quantum Fisher information of $\mathcal{E}(\rho_S)$, $\mathcal{F}(\mathcal{E}(\rho_S))$ is upper bounded by the optimal coarse grained measurement on ρ_E with the same number of outcomes as the dimension on ρ_S which we will denote by $F(\rho_E, G_i^*)$. Finally, we know that $F_{2|1=k'} = F(\mathcal{E}^{k'}(|k'\rangle\langle k'|), |k\rangle\langle k|)$ which implies

$$\begin{aligned}
F_{2|1} &= \sum_{k'} q_{k'} F_{2|1=k'} \leq \sum_{k'} q_{k'} \mathcal{F}(\mathcal{E}^{k'}(|k'\rangle\langle k'|)) \\
&\leq \sum_{k'} q_{k'} F(\rho_E, G_i^*) = F(\rho_E, G_i^*).
\end{aligned} \tag{A.4}$$

This result is also interesting when the environment has a smaller dimension than the system such as might be the case in a collision model setup. In this case the Fisher information we can obtain from measuring the system is bounded by the quantum Fisher information of the environment, therefore larger probes are not necessarily more informative.

Appendix B. Exact solution of the sequential thermometry problem

In this appendix we give details on how to calculate the probabilities $P(k|k')$ for the metrology problem in equations (29)–(33). The system obeys the master equation (27), which forms the so-called Davies maps, which do not create coherences. Hence, the evolution after each measurement will remain diagonal and we can map this into a classical master equation problem. Define the D -dimensional transition matrix

$$W = \begin{pmatrix} -\gamma(D-1)\bar{n} & \gamma(\bar{n}+1) & \gamma(\bar{n}+1) & \dots \\ \gamma\bar{n} & -\gamma(\bar{n}+1) & 0 & \dots \\ \gamma\bar{n} & 0 & -\gamma(\bar{n}+1) & \dots \\ \vdots & \vdots & \vdots & \ddots \end{pmatrix}. \tag{B.1}$$

The transition probabilities will then be

$$P(k|k') = (e^{W\tau})_{kk'}, \tag{B.2}$$

where τ is the time between measurements.

To compute this matrix exponential we solve the corresponding master equation

$$\frac{dp_k}{dt} = \sum_{k'} W_{kk'} p_{k'}, \tag{B.3}$$

for all initial conditions of the form $p_k(0) = \delta_{k,i}$. We proceed in 2 steps. First, define $p_e = \sum_{i=1}^{D-1} q_i$. Then, because of the symmetry of the problem, we can actually solve a simple 2-dimensional equation for p_0 and p_e :

$$\frac{dp_0}{dt} = \gamma(\bar{n}+1)p_e - \gamma(D-1)\bar{n}p_0, \tag{B.4}$$

$$\frac{dp_e}{dt} = \gamma(D-1)\bar{n}p_0 - \gamma(\bar{n}+1)p_e. \tag{B.5}$$

The solution is

$$p_0(t) = (q_0 + q_e f) p_0(0) + q_0(1-f) p_e(0), \tag{B.6}$$

$$p_e(t) = q_e(1-f) p_0(0) + (q_e + q_0 f) p_e(0), \tag{B.7}$$

where $f = e^{-\gamma t(D\bar{n}+1)}$. From this we can already read off $P(0|0)$ in equation (29), as being the coefficient in equation (B.6) that multiplies $p_0(0)$. Similarly, because $p_e(0) = \sum_{i=1}^{D-1} p_i(0)$, we can also read off from equation (B.6) the element $P(0|i)$.

For the remaining elements we need to determine the probabilities of the individual states p_i . From the master equation (B.3) we have that

$$\frac{dp_i}{dt} = -\gamma(\bar{n}+1)p_i + \gamma\bar{n}p_0(t). \quad (\text{B.8})$$

Since $p_0(t)$ is known the solution will be

$$p_i(\tau) = gp_i(0) + \gamma\bar{n} \int_0^\tau dt' g(\tau-t') \left[(q_0 + q_e f(t'))p_0(0) + q_0(1-f(t')) \left(\sum_{i=1}^{D-1} p_i(0) \right) \right], \quad (\text{B.9})$$

where $g \equiv g(\tau) = e^{-\gamma\tau(\bar{n}+1)}$. The remaining matrix elements $(e^{Wt})_{kk'}$ can now all be directly read off from these results. For example, the element $P(i|0)$ is read from equation (B.9) by looking at all terms that multiply $p_0(0)$. Carrying out the time integrals we obtain the results in equations (29)–(33).

This analysis also shows why the thermal probabilities q_k are still steady-states of the Markov process, even if τ is finite. Namely, since $W\mathbf{q} = 0$, it follows that $e^{Wt}\mathbf{q} = \mathbf{q}$.

ORCID iDs

Eoin O'Connor  <https://orcid.org/0000-0002-8900-6649>

Steve Campbell  <https://orcid.org/0000-0002-3427-9113>

Gabriel T Landi  <https://orcid.org/0000-0001-8451-9712>

References

- [1] Cramér H 1999 *Mathematical Methods of Statistics* vol 43 (Princeton University Press)
- [2] Rao C R 1973 *Linear Statistical Inference and its Applications* vol 2 (Wiley)
- [3] Fisher R A 1922 On the mathematical foundations of theoretical statistics *Phil. Trans. R. Soc. A* **222** 309–68
- [4] Giovannetti V, Lloyd S and Maccone L 2004 Quantum-enhanced measurements: beating the standard quantum limit *Science* **306** 1330–6
- [5] Giovannetti V, Lloyd S and Maccone L 2006 Quantum metrology *Phys. Rev. Lett.* **96** 010401
- [6] Giovannetti V, Lloyd S and Maccone L 2011 Advances in quantum metrology *Nat. Photon.* **5** 222–9
- [7] Braun D, Adesso G, Benatti F, Floreanini R, Marzolino U, Mitchell M W and Pirandola S 2018 Quantum-enhanced measurements without entanglement *Rev. Mod. Phys.* **90** 035006
- [8] Frérot I and Roscilde T 2018 Quantum critical metrology *Phys. Rev. Lett.* **121** 020402
- [9] Rams M M, Sierant P, Dutta O, Horodecki P and Zakrzewski J 2018 At the limits of criticality-based quantum metrology: apparent super-heisenberg scaling revisited *Phys. Rev. X* **8** 021022
- [10] Garbe L, Abah O, Felicetti S and Puebla R 2022 Exponential time-scaling of estimation precision by reaching a quantum critical point *Phys. Rev. Res.* **4** 043061
- [11] Yu M, Nguyen H C and Nimmrichter S Criticality-enhanced precision in phase thermometry (arXiv:2311.14578 [quant-ph])
- [12] Hotter C, Ritsch H and Gietka K 2024 Combining critical and quantum metrology *Phys. Rev. Lett.* **132** 060801
- [13] Ostermann L and Gietka K 2023 Temperature-enhanced critical quantum metrology (arXiv:2312.04176 [quant-ph])
- [14] Mihailescu G, Bayat A, Campbell S and Mitchell A K 2023 Multiparameter critical quantum metrology with impurity probes (arXiv:2311.16931 [quant-ph])
- [15] Braginsky V B and Khalili F Y 1995 *Quantum Measurement* (Cambridge University Press)
- [16] Busch P, Cassinelli P J and Lahti G 1990 On the quantum theory of sequential measurements *Found. Phys.* **20** 757–75
- [17] Wiseman H M 1995 Using feedback to eliminate back-action in quantum measurements *Phys. Rev. A* **51** 2459
- [18] Gudder S and Nagy G 2001 Sequential quantum measurements *J. Math. Phys.* **42** 5212–22
- [19] Naik A, Buu O, LaHaye M D, Armour A D, Clerk A A, Blencowe M P and Schwab K C 2006 Cooling a nanomechanical resonator with quantum back-action *Nature* **443** 193–6
- [20] Hatridge M et al 2013 Quantum back-action of an individual variable-strength measurement *Science* **339** 178–81
- [21] Nagali E, Felicetti S, de Assis P-L, D'Ambrosio V, Filip R and Sciarrino F 2012 Testing sequential quantum measurements: how can maximal knowledge be extracted? *Sci. Rep.* **2** 443
- [22] Küllerich A H and Mølmer K 2015 Quantum zeno effect in parameter estimation *Phys. Rev. A* **92** 032124
- [23] Burgarth D, Giovannetti V, Kato A N and Yuasa K 2015 Quantum estimation via sequential measurements *New J. Phys.* **17** 113055
- [24] Müller M M, Gherardini S, Smerzi A and Caruso F 2016 Fisher information from stochastic quantum measurements *Phys. Rev. A* **94** 042322
- [25] De Pasquale A, Yuasa K and Giovannetti V 2017 Estimating temperature via sequential measurements *Phys. Rev. A* **96** 012316
- [26] Bompais M and Amini N H 2023 On asymptotic stability of non-demolition quantum trajectories with measurement imperfections (arXiv:2304.02462 [quant-ph])
- [27] Clark L A, Stokes A and Beige A 2019 Quantum jump metrology *Phys. Rev. A* **99** 022102
- [28] Montenegro V, Jones G S, Bose S and Bayat A 2022 Sequential measurements for quantum-enhanced magnetometry in spin chain probes *Phys. Rev. Lett.* **129** 120503

- [29] Yang Y, Montenegro V and Bayat A 2023 Extractable information capacity in sequential measurements metrology (arXiv:2308.03370)
- [30] Radaelli M, Landi G T, Modi K and Binder F C 2023 Fisher information of correlated stochastic processes *New J. Phys.* **25** 053037
- [31] Smiga J A, Radaelli M, Binder F C and Landi G T 2023 Stochastic metrology and the empirical distribution *Phys. Rev. Res.* **5** 033150
- [32] Gammelmark S and Mølmer K 2013 Bayesian parameter inference from continuously monitored quantum systems *Phys. Rev. A* **87** 032115
- [33] Gammelmark S and Mølmer K 2014 Fisher information and the quantum cramer-rao sensitivity limit of continuous measurements *Phys. Rev. Lett.* **112** 170401
- [34] Küllerich A H and Mølmer K 2016 Bayesian parameter estimation by continuous homodyne detection *Phys. Rev. A* **94** 032103
- [35] Genoni M G 2017 Cramer-rao bound for time-continuous measurements in linear gaussian quantum systems *Phys. Rev. A* **95** 012116
- [36] Albarelli F, Rossi M A C, Paris M G A and Genoni M G 2017 Ultimate limits for quantum magnetometry via time-continuous measurements *New J. Phys.* **19** 123011
- [37] Albarelli F, Rossi M A C, Tamascelli D and Genoni M G 2018 Restoring heisenberg scaling in noisy quantum metrology by monitoring the environment *Quantum* **2** 110
- [38] Rossi M A C, Albarelli F, Tamascelli D and Genoni M G 2020 Noisy quantum metrology enhanced by continuous nondemolition measurement *Phys. Rev. Lett.* **125** 200505
- [39] Ashhab S, You J Q and Nori F 2009 The information about the state of a qubit gained by a weakly coupled detector *New J. Phys.* **11** 083017
- [40] Ashhab S, You J Q and Nori F 2009 Weak and strong measurement of a qubit using a switching-based detector *Phys. Rev. A* **79** 032317
- [41] Radaelli M, Smiga J A, Landi G T and Binder F C 2024 Parameter estimation for quantum jump unraveling (arXiv:2402.06556)
- [42] Wiseman H M and Milburn G J 2009 *Quantum Measurement and Control* (Cambridge University Press)
- [43] Zhang J, Liu Y, Wu R-B, Jacobs K and Nori F 2017 Quantum feedback: theory, experiments and applications *Phys. Rep.* **679** 1–60
- [44] Guță M 2011 Fisher information and asymptotic normality in system identification for quantum markov chains *Phys. Rev. A* **83** 062324
- [45] Cătană C, van Horsen M and Guță M 2012 Asymptotic inference in system identification for the atom maser *Phil. Trans. R. Soc. A* **370** 5308–23
- [46] Ciccarello E, Lorenzo S, Giovannetti V and Palma M G 2022 Quantum collision models: Open system dynamics from repeated interactions *Phys. Rep.* **954** 1–70
- [47] Campbell S and Vacchini B 2021 Collision models in open system dynamics: a versatile tool for deeper insights? *Europhys. Lett.* **133** 60001
- [48] Hovhannisyán K V, Jørgensen M R, Landi G T, Alhambra A M, Brask J B and Perarnau-Llobet M 2021 Optimal quantum thermometry with coarse-grained measurements *PRX Quantum* **2** 020322
- [49] Seah S, Nimmrichter S, Grimmer D, Santos J P, Scarani V and Landi G T 2019 Collisional quantum thermometry *Phys. Rev. Lett.* **123** 180602
- [50] Shu A, Seah S and Scarani V 2020 Surpassing the thermal Cramer–Rao bound with collisional thermometry *Phys. Rev. A* **102** 042417
- [51] Alves G O and Landi G T 2022 Bayesian estimation for collisional thermometry *Phys. Rev. A* **105** 012212
- [52] O'Connor E, Vacchini B and Campbell S 2021 Stochastic collisional quantum thermometry *Entropy* **23** 1634
- [53] Gelfand I and Neumark M 1943 On the imbedding of normed rings into the ring of operators in hilbert space *Rec. Math. [Mat. Sbornik] N.S.* **12** 197–217
- [54] De Pasquale A and Stace T M 2018 Quantum thermometry *Thermodynamics in the Quantum Regime* (Springer) pp 503–27
- [55] Razavian S, Benedetti C, Bina M, Akbari-Kourbolagh Y and Paris M G A 2019 Quantum thermometry by single-qubit dephasing *Eur. Phys. J. Plus* **134** 284
- [56] Mehboudi M, Sanpera A and Correa L A 2019 Thermometry in the quantum regime: recent theoretical progress *J. Phys. A: Math. Theor.* **52** 303001
- [57] Mitchison M T, Fogarty T, Guarnieri G, Campbell S, Busch T and Goold J 2020 In situ thermometry of a cold fermi gas via dephasing impurities *Phys. Rev. Lett.* **125** 284
- [58] Brattegard S and Mitchison M T 2024 Thermometry by correlated dephasing of impurities in a one-dimensional fermi gas *Phys. Rev. A* **109** 023309
- [59] Mihailescu G, Campbell S and Mitchell A K 2023 Thermometry of strongly correlated fermionic quantum systems using impurity probes *Phys. Rev. A* **107** 042614
- [60] Mok W-K, Bharti K, Kwek L-C and Bayat A 2021 Optimal probes for global quantum thermometry *Commun. Phys.* **4** 62
- [61] Correa L A, Perarnau-Llobet M, Hovhannisyán K V, Hernández-Santana S, Mehboudi M and Sanpera A 2017 Enhancement of low-temperature thermometry by strong coupling *Phys. Rev. A* **96** 062103
- [62] Hovhannisyán K V and Correa L A 2018 Measuring the temperature of cold many-body quantum systems *Phys. Rev. B* **98** 045101
- [63] Potts P P, Brask J B and Brunner N 2019 Fundamental limits on low-temperature quantum thermometry with finite resolution *Quantum* **3** 161
- [64] Correa L A, Mehboudi M, Adesso G and Sanpera A 2015 Individual quantum probes for optimal thermometry *Phys. Rev. Lett.* **114** 220405